

# RPS25 is required for efficient RAN translation of *C9orf72* and other neurodegenerative disease-associated nucleotide repeats

Shizuka B. Yamada<sup>1,2</sup>, Tania F. Gendron<sup>3</sup>, Teresa Niccoli<sup>4,5,6</sup>, Naomi R. Genuth<sup>1,2,7</sup>, Rosslyn Grosely<sup>8</sup>, Yingxiao Shi<sup>9</sup>, Idoia Glaria<sup>4,5</sup>, Nicholas J. Kramer<sup>1,10</sup>, Lisa Nakayama<sup>1</sup>, Shirleen Fang<sup>1</sup>, Tai J. I. Dinger<sup>1,2</sup>, Annora Thoeng<sup>4,5,6</sup>, Gabriel Rocha<sup>9</sup>, Maria Barna<sup>1,7</sup>, Joseph D. Puglisi<sup>8</sup>, Linda Partridge<sup>6</sup>, Justin K. Ichida<sup>9</sup>, Adrian M. Isaacs<sup>4,5</sup>, Leonard Petrucelli<sup>3</sup> and Aaron D. Gitler<sup>1\*</sup>

**Nucleotide repeat expansions in the *C9orf72* gene are the most common cause of amyotrophic lateral sclerosis and frontotemporal dementia. Unconventional translation (RAN translation) of *C9orf72* repeats generates dipeptide repeat proteins that can cause neurodegeneration. We performed a genetic screen for regulators of RAN translation and identified small ribosomal protein subunit 25 (RPS25), presenting a potential therapeutic target for *C9orf72*-related amyotrophic lateral sclerosis and frontotemporal dementia and other neurodegenerative diseases caused by nucleotide repeat expansions.**

The most common genetic cause of amyotrophic lateral sclerosis (ALS) and frontotemporal dementia (FTD) is a mutation in the *C9orf72* gene<sup>1,2</sup>. The mutation is an expansion of the repetitive nucleotide tract GGGGCC within the first intron of *C9orf72*. The expanded nucleotide repeat is translated by an unconventional form of translation, called repeat-associated non-AUG (RAN) translation to produce dipeptide repeat (DPR) proteins<sup>3–7</sup>. These DPRs are aggregation prone, accumulate in the central nervous system of patients and could cause disease through a protein toxicity mechanism. Insight into the mechanism of RAN translation requires analysis of the sequence features promoting RAN translation<sup>8–10</sup> and the identification of regulators.

We discovered that RAN translation occurs in yeast (Fig. 1a), indicating that it exploits an evolutionarily conserved process or machinery and, importantly, providing the opportunity to discover genes required for this process. We designed a genetic screen to identify genes that specifically affected RAN translation, but not GGGGCC-repeat RNA levels or general translation (Fig. 1b). We assembled a library of 275 yeast mutants for genes encoding translational machinery, including ribosomal subunits and other translation factors (see Supplementary Table 1). We introduced a galactose-inducible *C9orf72* 66 repeat construct into each strain by transformation and used a poly(GP) immunoassay to gauge levels of RAN translation. To identify hits that specifically affected RAN translation and not general translation, we counter-screened hits by assessing their effect on the expression of an

ATG-initiated green fluorescent protein (GFP) construct. We identified 42 genes that either increased or decreased DPR levels without similarly regulating ATG–GFP (Fig. 1c and see Supplementary Fig. 1a–c). We also performed quantitative PCR with reverse transcription (RT–qPCR) to identify hits that affected transcription or RNA stability of the repeat RNA (see Supplementary Table 1).

One striking hit from the screen was the deletion of *RPS25A*, which encodes a eukaryotic-specific, non-essential protein component of the small (40S) ribosomal subunit<sup>11,12</sup>. RPS25 plays a critical role in several forms of unconventional translation including internal ribosome entry site (IRES)-mediated translation and ribosomal shunting<sup>13</sup>. RPS25 mediates the direct recruitment of the 40S ribosomal subunit to the cricket paralysis virus IRES RNA. It also regulates translation initiation of hepatitis C virus and picornaviral IRES RNAs, downstream of 40S subunit recruitment<sup>11–14</sup>. In addition to viral RNAs, RPS25 regulates several cellular IRES-containing RNAs including p53 and *c-myc*<sup>13,15</sup>. Deleting *RPS25A* (*rps25Δ*) reduced levels of RAN-translated poly(GP) by 50% compared with wild-type (WT) yeast (Fig. 1c,d). Deletion of *RPS25A* did not affect the levels of GFP or the abundance of GGGGCC-repeat RNA (see Supplementary Fig. 1d–f).

In mammals, there is a single RPS25 homolog, ribosomal protein S25 (RPS25). To test whether the function of RPS25 in RAN translation is conserved from yeast to human, we analyzed a human cell line (Hap1) that harbors a CRISPR-induced knockout (KO) of *RPS25* (ref. 12). We transfected a 66-repeat construct, analogous to the one used for the yeast experiments, into Hap1 *RPS25* KO cells. *RPS25* KO resulted in ~50% reduction in poly(GP) levels without affecting the levels of repeat RNA (Fig. 1e and see Supplementary Fig. 2a). As RAN translation can occur in multiple reading frames of the GGGGCC repeat, we also tested the effects of *RPS25* KO on another reading frame and found that the glycine–alanine (GA) frame was reduced by >90% compared with WT (Fig. 1f,g). Finally, we found that *RPS25* KO reduced glycine–arginine (GR) levels by ~30%, comparable to control cells not expressing the GGGGCC repeat (Fig. 1h and see Supplementary Fig. 2b).

<sup>1</sup>Department of Genetics, Stanford University School of Medicine, Stanford, CA, USA. <sup>2</sup>Department of Biology, Stanford University, Stanford, CA, USA.

<sup>3</sup>Department of Neuroscience, Mayo Clinic, Jacksonville, FL, USA. <sup>4</sup>Department of Neurodegenerative Disease, UCL Institute of Neurology, London, UK.

<sup>5</sup>UK Dementia Research Institute at UCL, UCL Institute of Neurology, London, UK. <sup>6</sup>Department of Genetics, Evolution and Environment, Institute of Healthy Ageing, University College London, London, UK. <sup>7</sup>Department of Developmental Biology, Stanford University School of Medicine, Stanford, CA, USA. <sup>8</sup>Department of Structural Biology, Stanford University School of Medicine, Stanford, CA, USA. <sup>9</sup>Department of Stem Cell Biology and Regenerative Medicine, Eli and Edythe Broad Center for Regenerative Medicine and Stem Cell Research, University of Southern California, Los Angeles, CA, USA.

<sup>10</sup>Stanford Neurosciences Graduate Program, Stanford University School of Medicine, Stanford, CA, USA. \*e-mail: [agitler@stanford.edu](mailto:agitler@stanford.edu)

The higher level of background poly(GR) signal in this immunoassay, even after *RPS25* KO, probably reflects the abundance of GR repeats in the proteome (for example, RGG/RG motifs)<sup>16</sup>.

To test the impact of *RPS25* KO on global translation, we performed puromycin-incorporation assays. Consistent with previous observations<sup>11,13</sup>, *RPS25* KO did not affect global translation (see Supplementary Fig. 2c–e). Furthermore, *RPS25* KO did not significantly alter cell growth rate or expression of a canonically translated ATG–clover reporter (see Supplementary Fig. 2f–j). *RPS25* KO had only mild effects on polysome profiles, a global measure of actively translated messenger RNAs (see Supplementary Fig. 3a,b). Notably, although nearly all profile peak:40S ratios remained similar, the 60S:40S and heavy polysome:40S ratios were increased in *RPS25* KO cells, providing evidence that global translation is not substantially impaired in *RPS25* KO cells. RT–qPCR analysis, from RNA associated with different fractions of the polysome profile, illustrated that there is no decrease in heavy polysome-associated (generally thought to be highly translated) *ACTB* or *GFP* (see Supplementary Fig. 3c,d). Importantly, there was less GGGGCC-repeat RNA associated with heavy polysomes in *RPS25* KO cells compared with WT (see Supplementary Fig. 3e), consistent with decreased translation of GGGGCC RNA in *RPS25* KO cells. These data are consistent with a role of *RPS25* in RAN translation of the *C9orf72* repeat expansion.

How generalizable is the effect of *RPS25* KO on RAN translation? Is *RPS25* required for efficient RAN translation of other nucleotide repeat expansions? First, we generated *ATXN2* CAG repeat constructs, mutating all ATG codons upstream of the CAG repeats and placing a myc/his tag in frame with poly(Ala) (poly(A)) RAN products (see Supplementary Fig. 4a,b). We then generated a HeLa cell line with a CRISPR-induced mutation in *RPS25*, which markedly reduces levels of *RPS25* (see Supplementary Fig. 4c–h). Consistent with other repeats, we only detected poly(A) and poly(Q) products in the longer *ATXN2* CAG repeat lengths (CAG58 and CAG108, Fig. 1i–k). Expression of both these reading frames was reduced in the *RPS25* mutant HeLa cell line (Fig. 1i–k and see Supplementary Fig. 4g–i). Next, we tested RAN translation of mutant huntingtin protein (HTT). *RPS25* reduction in HeLa cells reduces poly(A) RAN products expressed from unmodified *HTT* CAG repeats but does not significantly reduce the expression of poly(Q) that initiates from the native ATG codon of *HTT* (see Supplementary Fig. 4j–l

and Supplementary Table 2). Thus, *RPS25* is required for efficient RAN translation of both CAG and GGGGCC repeats.

To extend the findings of the present study to a more clinically relevant system, we next asked whether *RPS25* regulates RAN translation of *C9orf72* repeats expressed from their endogenous context and at physiological levels in cells obtained from humans with ALS. We analyzed cultured induced pluripotent stem cells (iPSCs) from two healthy subjects and three ALS patients with *C9orf72* repeat expansions. Reduction of *RPS25* levels by short interfering RNA (siRNA) substantially reduced the levels of poly(GP) compared with the non-targeting control (Fig. 2a,b, and see Supplementary Fig. 5a,b, and Supplementary Table 3). Importantly, *RPS25* reduction did not influence the number of RNA foci (Fig. 2c–e) or levels of the different *C9orf72* alternative transcript variants, including transcripts specifically harboring the GGGGCC repeat (Fig. 2f,g), indicating that *RPS25* functions at the level of translation without impacting repeat RNA transcription, stability or foci formation. *RPS25* reduction did not alter endogenous *C9orf72* protein expression (see Supplementary Fig. 5c). Thus, *RPS25* regulates the endogenous RAN translation of *C9orf72* nucleotide repeat expansions in the poly(GP) frame.

We next tested whether inhibition of *RPS25* could mitigate neurodegenerative phenotypes caused by *C9orf72* repeat expansions in vivo. We used transgenic *Drosophila*, engineered to express 36 GGGGCC repeats under the control of the inducible elav-GeneSwitch driver. Consistent with previous reports<sup>17</sup>, neuronal expression of 36 repeats resulted in the production of DPRs (Fig. 3a,b) and shortened lifespan (Fig. 3c). Reducing the expression of *Drosophila* Rps25 using RNA interference (RNAi) lowered poly(GP) levels (Fig. 3a,b and see Supplementary Fig. 6) and substantially increased the lifespan of 36 repeat-expressing, adult, male flies (Fig. 3c and see Supplementary Fig. 7a,e,g). Notably, as a control, we reduced Rps25 in flies engineered to express 36 GR dipeptide codon-optimized repeats driven from an ATG (36GR) and not in the context of a repetitive GGGGCC tract<sup>17</sup>, and therefore these do not undergo RAN translation. Reducing Rps25 levels did not rescue the shortened lifespan of 36GR flies (Fig. 3d), providing evidence that Rps25 functions upstream or at the level of production of the toxic DPRs. Rps25 RNAi did not affect the lifespan of WT male flies (Fig. 3c and Supplementary Fig. 7f). Thus, Rps25 is required for RAN translation in the poly(GP)

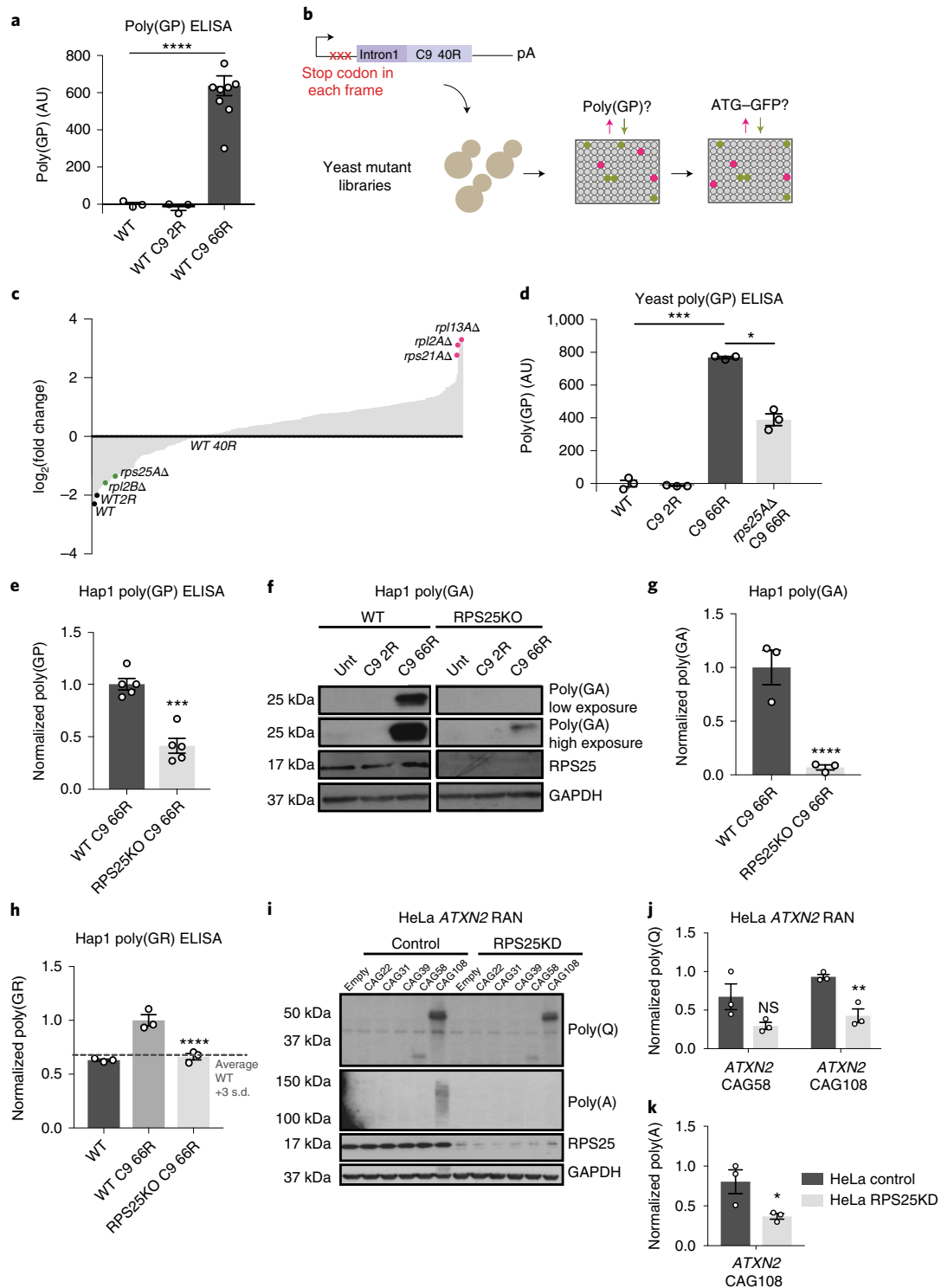
**Fig. 1 | *RPS25* is required for efficient RAN translation in yeast and human cells.** **a**, Detection of RAN-translated DPR in yeast lysate using a poly(GP) immunoassay. WT (BY4741) yeast were transformed with an empty vector or constructs expressing either 2 or 66 *C9orf72* GGGGCC repeats (C9 2R or 66R) under the control of a galactose-inducible promoter. DPR production was assayed in yeast lysates using a poly(GP) immunoassay. We detected poly(GP) in the C9 66R-expressing yeast (two-tailed, unpaired Student's *t*-test;  $n = 3$  WT and WT C9 2R transformations;  $n = 8$  independent *rps25Δ* C9 66R transformations; \*\*\*\* $P < 0.0001$ ; mean  $\pm$  s.e.m.). **b**, Schematic of yeast poly(GP) and ATG–GFP counter-screen to identify RAN translation regulators. C9 40R expression constructs were introduced by transformation or mating into yeast mutants from the deletion collection (MATa; non-essential genes) and DAMP library (essential genes). Mutants were assayed for poly(GP) levels using a poly(GP) immunoassay and counter-screened with a GFP immunoassay. Data are provided in Supplementary Table 1. **c**, Fold-change poly(GP) levels of yeast mutants compared with WT yeast expression ( $n = 3$  independent transformations for each strain). **d**, Independent validation of *rps25Δ* mutant expressing C9 66R using poly(GP) immunoassay. Poly(GP) levels were approximately 50% lower in *rps25Δ* compared with WT yeast (two-tailed, unpaired Student's *t*-test;  $n = 3$  independent deletion strains; \*\*\* $P = 0.0010$ , \* $P = 0.0248$ ; mean  $\pm$  s.e.m.). AU, arbitrary units. **e**, Immunoassay showing that *RPS25* knockout (KO) in the human Hap1 cell line reduces poly(GP) levels (two-tailed, unpaired Student's *t*-test;  $n = 5$  independent cell culture experiments; \*\*\* $P = 0.0002$ ; mean  $\pm$  s.e.m.). **f**, Lysates from transfected Hap1 cells immunoblotted for poly(GA) expression (HA-epitope tag). **g**, Quantification of **f** (uncropped blots for this and all subsequent blots can be found in Supplementary Fig. 11; two-tailed, unpaired Student's *t*-test;  $n = 3$  independent cell culture experiments; \*\*\*\* $P < 0.0001$ ; mean  $\pm$  s.e.m.). **h**, Immunoassay showing that *RPS25* KO in Hap1 cells reduces poly(GR) levels to that of Hap1 WT transfected with empty vector. Full conditions and ANOVA statistics are shown in Supplementary Fig. 3 (ordinary one-way ANOVA with Tukey's multiple comparisons;  $n = 3$  independent cell culture experiments; \*\*\*\* $P < 0.0001$ ; mean  $\pm$  s.e.m.). **i**, Lysates from transfected HeLa cells immunoblotted for poly(Q) and poly(A) *ATXN2* RAN products. **j,k**, Quantification where poly(Q) or poly(A) is normalized to GAPDH (**i**). **j**, *ATXN2* CAG108 RAN-translated poly(Q) products are reduced in HeLa cells harboring a CRISPR-induced mutation that markedly reduces protein level of *RPS25* (*RPS25* knockdown (KD)) compared with HeLa control cell (two-tailed, unpaired Student's *t*-test;  $n = 3$  independent cell culture experiments; \*\* $P = 0.0059$ ; NS, not significant  $P = 0.0946$ ; mean  $\pm$  s.e.m.). **k**, *ATXN2* CAG108 RAN poly(A) products are reduced in HeLa *RPS25* KD mutant compared with HeLa control (two-tailed, unpaired Student's *t*-test;  $n = 3$  independent cell culture experiments; \* $P = 0.0473$ ; mean  $\pm$  s.e.m.). Additional statistical details for this figure and subsequent figures are provided in Supplementary Table 4 and the Methods.

frame and the pathogenicity of *C9orf72* GGGGCC repeats in the nervous system of *Drosophila*.

Finally, to extend the studies of the present study to human neurons, we tested the impact of lowering *RPS25* levels on survival phenotypes in motor neurons from patients with ALS harboring endogenous *C9orf72* GGGGCC expansions. We used transcription factor-mediated reprogramming to generate induced motor neurons (iMNs) from iPSCs of patients with *C9orf72* ALS and unaffected individuals, as previously described<sup>18</sup>. The c9ALS patient-derived iMNs showed reduced survival after glutamate addition compared with control iMNs (Fig. 3e and see Supplementary Fig. 8c,f,i).

We tested two independent antisense oligonucleotides (ASOs) that targeted *RPS25* with one non-targeting control ASO. Both *RPS25* ASOs substantially increased the proportion of surviving iMNs in the c9ALS line (Fig. 3e, and see Supplementary Figs. 8c,f,i and 8a), but did not increase survival of control iMNs (see Supplementary Fig. 8b). Furthermore, both *RPS25* ASOs significantly reduced the number of poly(GR) and poly(PR) foci in c9ALS patient-derived iMNs (Fig. 3f,g, and see Supplementary Figs. 8d,e,g,h,j,k, 9 and 10).

In the present study, we found that *RPS25* is selectively required for the efficient RAN translation of expanded GGGGCC repeat expansions in the *C9orf72* gene and CAG expansions



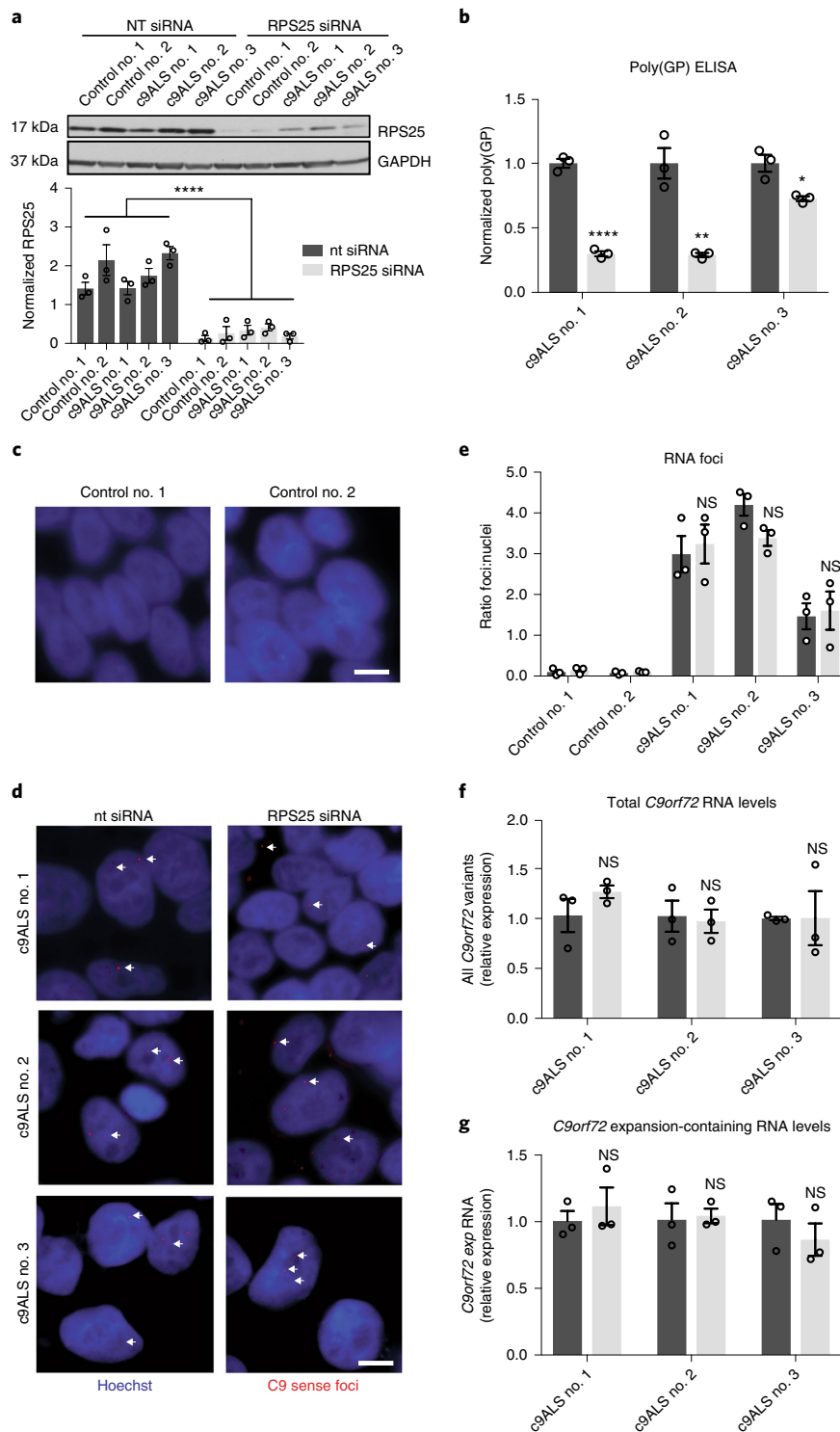


**Fig. 2 | RPS25 knockdown reduces poly(GP) levels in *C9orf72* ALS patient iPSCs.** Control and *c9ALS* patient-derived iPSCs were treated with non-targeting control siRNA or RPS25-targeting siRNA. **a**, Lysates from iPSCs treated with non-targeting or RPS25-targeting siRNAs immunoblotted for RPS25 expression. Quantification illustrates that RPS25 is reduced in RPS25-targeting siRNAs (one-way ANOVA with Tukey's multiple comparisons;  $n=3$  independent cell culture experiments per iPSC line and condition; \*\*\*\* $P<0.0001$ ; mean  $\pm$  s.e.m.). nt, nucleotide. **b**, Immunoassay for poly(GP) levels in *c9ALS* iPSCs showing reduction of poly(GP) levels in RPS25 siRNA-treated cells (two-tailed, unpaired Student's  $t$ -test;  $n=3$  independent cell culture experiments per iPSC line and condition; \*\*\*\* $P<0.0001$ , \*\* $P=0.0039$ , \* $P=0.0161$ ; mean  $\pm$  s.e.m.) (see also Supplementary Fig. 5b). **c,d**, RNA FISH with probe for GGGGCC (sense) RNA used to detect and quantify sense-repeat foci, pseudocolored in red. Cell nuclei are indicated in blue (Hoechst 33258). Scale bar,  $5\mu\text{m}$ . **c**, Control iPSCs derived from healthy subjects. **d**, *c9ALS* patient-derived iPSCs. **e**, Quantification of normalized foci per nuclei (two-tailed, unpaired Student's  $t$ -test;  $n=3$  independent cell culture experiments; NS, not significant: *c9ALS* no. 1,  $P=0.7234$ ; *c9ALS* no. 2,  $P=0.0654$ ; *c9ALS* no. 3,  $P=0.8189$ ; mean  $\pm$  s.e.m.). **f**, RT-qPCR of total *C9orf72* mRNA (two-tailed, unpaired Student's  $t$ -test;  $n=3$  independent cell culture experiments; NS, not significant: *c9ALS* no. 1,  $P=0.2509$ ; *c9ALS* no. 2,  $P=0.8068$ ; *c9ALS* no. 3,  $P=0.9912$ ; mean  $\pm$  s.e.m.). **g**, RT-qPCR of *C9orf72* mRNA variants harboring the repeat expansion (exp) (two-tailed, unpaired Student's  $t$ -test;  $n=3$  independent cell culture experiments; NS, not significant: *c9ALS* no. 1,  $P=0.5289$ ; *c9ALS* no. 2,  $P=0.8390$ ; *c9ALS* no. 3,  $P=0.4279$ ; mean  $\pm$  s.e.m.).

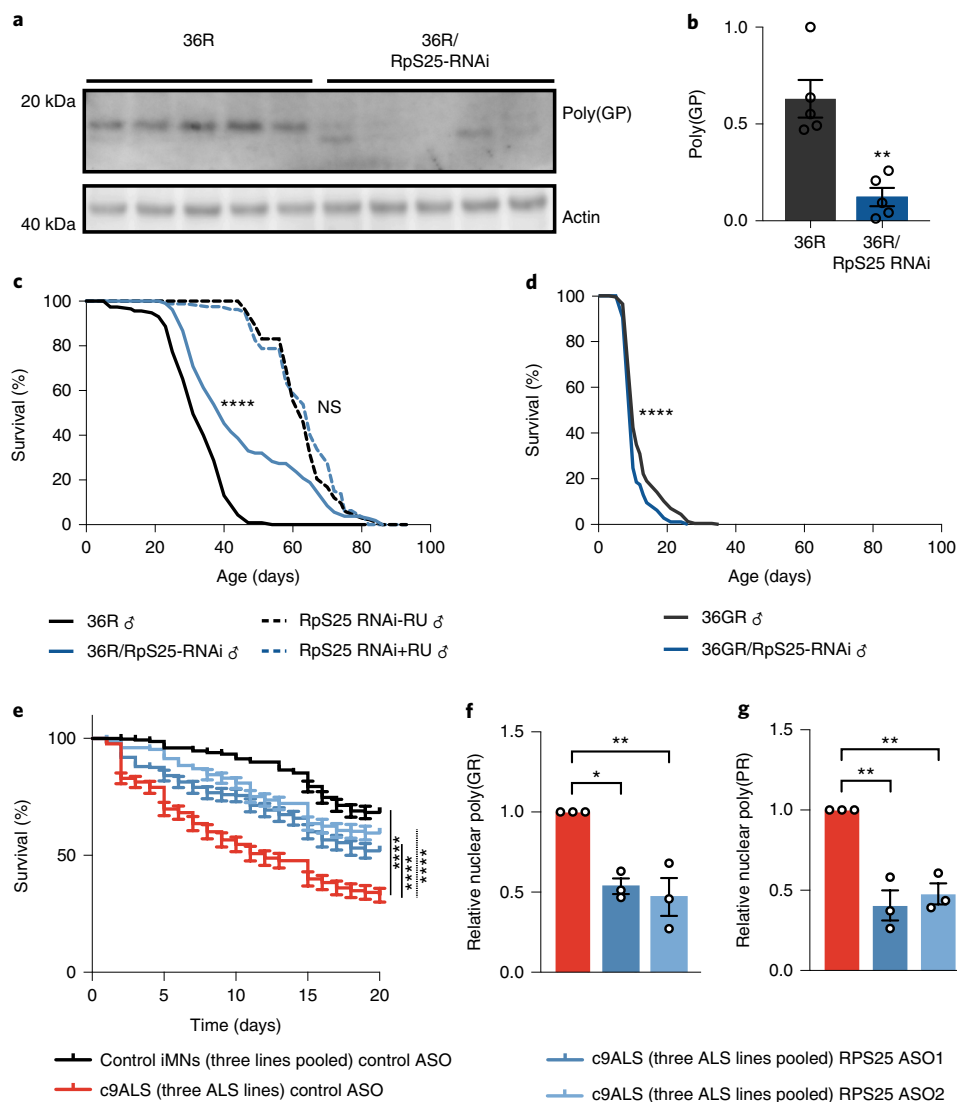


**Fig. 3 | RPS25 knockdown reduces RAN translation products and extends lifespan in a *Drosophila* C9orf72 model and in ALS patient-derived iMNs.**

**a**, Immunoblot of fly heads expressing 36(GGGGCC) (36R) alone or together with Rps25 RNAi in adult neurons, showing a reduction of poly(GP) levels in 36R flies expressing Rps25 RNAi. Genotypes: *UAS-36(GGGGCC)/+*; *elavGS*, *UAS-36(GGGGCC)/Rps25RNAi{KK107958}*; *elavGS/+*. **b**, Quantification of blots in **a** (two-tailed, unpaired Student's *t*-test; *n* = 5 biological replicates; \*\**P* = 0.0015). **c**, Survival curves of male ( $\delta$ ) flies expressing an inducible 36(GGGGCC) construct alone or together with Rps25 RNAi. Rps25 RNAi resulted in a lifespan increase in the 36R flies ( $\chi^2$  log-rank test; \*\*\*\**P* < 0.0001). Median lifespans: C9 36R flies, 29 days; C9 36R/Rps25 RNAi, 38 days. Genotypes and *n*: *UAS-36(GGGGCC)/+*; *elavGS* (*n* = 115 flies), *UAS-36(GGGGCC)/Rps25RNAi{KK107958}*; *elavGS/+* (*n* = 106 flies). In separate analyses, flies expressing Rps25 RNAi alone did not alter lifespan ( $\chi^2$  log-rank test; *n* = 83 uninduced, *n* = 80 RNAi induced; NS, not significant *P* = 0.4766). Median lifespans: Rps25 RNAi uninduced, 59 days; Rps25 RNAi induced, 61 days. Genotype: *UAS-Rps25RNAi{KK107958}/+*; *elavGS/+*. **d**, Expression of Rps25 RNAi together with 36GR repeats decreases survival of male flies ( $\chi^2$  log-rank test; \*\*\*\**P* < 0.0001). Genotypes: *UAS-36GR/+*; *elavGS* (*n* = 226 flies), *UAS-36GR/Rps25RNAi{KK107958}*; *elavGS/+* (*n* = 180 flies). The 36R flies are codon optimized, driven by AUG and do not undergo RAN translation. **e**, Quantification of surviving iMNs derived from c9ALS iPSC line nos. 4–6 and three control iPSC lines treated with RPS25-targeting ASO1 and ASO2 or ASO control. The survival of HB9-RFP + iMNs was tracked by imaging after addition of 10  $\mu$ M glutamate. Treatment of RPS25 ASO1 and ASO2 significantly increased survival of three c9ALS iMN lines (log-rank tests; *n* = 3 independent iMN lines per condition per treatment; \*\*\*\**P* < 0.0001; error bars, s.e.m.). **f**, Relative nuclear poly(GR) quantification of three c9ALS iMN lines treated with control or RPS25-targeting ASOs (one-way ANOVA with Tukey's multiple comparison; *n* = 3 independent iMN lines per condition per treatment with 20 iMNs analyzed and averaged for each *n*; \*\**P* = 0.0055, \**P* = 0.0105; mean  $\pm$  s.e.m.). **g**, Relative nuclear poly(PR) quantification of three c9ALS iMN lines treated with control or RPS25-targeting ASOs (one-way ANOVA with Tukey's multiple comparison; *n* = 3 independent iMN lines per condition per treatment with 20 iMNs analyzed and averaged for each *n*: ASO1, \*\**P* = 0.0017; ASO2, \*\**P* = 0.0034; mean  $\pm$  s.e.m.). For **f** and **g**, individual data per c9ALS iMN line can be found in Supplementary Fig. 8 and representative immunocytochemistry can be found in Supplementary Fig. 10.

in *ATXN2* and *HTT*. We present a novel protein involved in RAN translation and suggest that strategies to inhibit the function of RPS25 could be pursued as a therapy for c9ALS/FTD and perhaps other neurodegenerative diseases caused by nucleotide repeat expansions<sup>19,20</sup>.

#### Online content

Any methods, additional references, Nature Research reporting summaries, source data, statements of code and data availability and associated accession codes are available at <https://doi.org/10.1038/s41593-019-0455-7>.

Received: 10 September 2018; Accepted: 20 June 2019;  
Published online: 29 July 2019

## References

1. Renton, A. E. et al. *Neuron* **72**, 257–268 (2011).
2. DeJesus-Hernandez, M. et al. *Neuron* **72**, 245–256 (2011).
3. Mori, K. et al. *Science* **339**, 1335–1338 (2013).
4. Ash, P. E. et al. *Neuron* **77**, 639–646 (2013).
5. Zu, T. et al. *Proc. Natl Acad. Sci. USA* **110**, E4968–E4977 (2013).
6. Gendron, T. F. et al. *Acta Neuropathol.* **126**, 829–844 (2013).
7. Gao, F. B., Richter, J. D. & Cleveland, D. W. *Cell* **171**, 994–1000 (2017).
8. Cheng, W. et al. *Nat. Commun.* **9**, 51 (2018).
9. Green, K. M. et al. *Nat. Commun.* **8**, 2005 (2017).
10. Tabet, R. et al. *Nat. Commun.* **9**, 152 (2018).
11. Landry, D. M., Hertz, M. I. & Thompson, S. R. *Genes Dev.* **23**, 2753–2764 (2009).
12. Fuchs, G. et al. *Proc. Natl Acad. Sci. USA* **112**, 319–325 (2015).
13. Hertz, M. I., Landry, D. M., Willis, A. E., Luo, G. & Thompson, S. R. *Mol. Cell Biol.* **33**, 1016–1026 (2013).
14. Nishiyama, T., Yamamoto, H., Uchiyama, T. & Nakashima, N. *Nucleic Acids Res.* **35**, 1514–1521 (2007).
15. Shi, Y. et al. *Oncogene* **35**, 1015–1024 (2016).
16. Thandapani, P., O'Connor, T. R., Bailey, T. L. & Richard, S. *Mol. Cell* **50**, 613–623 (2013).
17. Mizielinska, S. et al. *Science* **345**, 1192–1194 (2014).
18. Shi, Y. et al. *Nat. Med.* **24**, 313–325 (2018).
19. Cleary, J. D. & Ranum, L. P. *Curr. Opin. Genet. Dev.* **44**, 125–134 (2017).
20. Green, K. M., Linsalata, A. E. & Todd, P. K. *Brain Res.* **1647**, 30–42 (2016).

## Acknowledgements

This work was supported by National Institutes of Health (NIH) grants nos. R35NS097263 (A.D.G.), AI099506 (J.D.P.), AG064690 (A.D.G. and J.D.P.), R35NS097273 (L.P.), P01NS099114 (T.F.G., L.P.) and R01NS097850 (J.K.I.), the Robert Packard Center for ALS Research at Johns Hopkins (L.P., A.D.G.), Target ALS (L.P., A.D.G., T.F.G.), the US Department of Defense (J.D.P., A.D.G., J.K.I.), the Muscular Dystrophy Association (J.K.I.),

2T32HG000044-21 NIHGRI training grant (S.B.Y.), the Brain Rejuvenation Project of the Wu Tsai Neurosciences Institute (A.D.G.), the European Research Council grant no. ERC-2014-CoG-648716 (A.M.I.), Alzheimer's Research UK (A.M.I.) and the Medical Research Council (A.M.I.). J.K.I. is supported by funding for a New York Stem Cell Foundation-Robertson Investigatorship. We thank Dr. L. Ranum (University of Florida) for sharing the huntingtin poly(alanine) antibody. We thank M. Bassik for the HeLa Cas9-BFP cell lines. We thank H. Tricoire (French National Center for Scientific Research) for the generous gift of the original elavGS 301.2 line.

## Author contributions

This work was performed and the paper written by S.B.Y. under the mentorship of A.D.G. T.F.G. contributed ELISA assays to detect RAN peptides and analyses under the mentorship of L.P., T.N., I.G. and A.T. contributed *Drosophila* studies under the mentorship of L.P. and A.M.I. N.R.G. contributed to polysome profiling studies and analyses, under the mentorship of M.B. R.G. contributed to RAN translation studies and analyses, under the mentorship of J.D.P. Y.S. and G.R. contributed induced motor neuron studies and analyses, under the mentorship of J.K.I. N.J.K. contributed to studies of *ATXN2* RAN translation. L.N., S.F. and T.J.I.D. contributed to studies of *C9orf72* RAN translation.

## Competing interests

A.D.G. has served as a consultant for Aquinnah Pharmaceuticals, Prevail Therapeutics and Third Rock Ventures and is a scientific founder of Maze Therapeutics.

## Additional information

**Supplementary information** is available for this paper at <https://doi.org/10.1038/s41593-019-0455-7>.

**Reprints and permissions information** is available at [www.nature.com/reprints](http://www.nature.com/reprints).

**Correspondence and requests for materials** should be addressed to A.D.G.

**Peer review information:** *Nature Neuroscience* thanks D. Dormann and the other, anonymous, reviewer(s) for their contribution to the peer review of this work.

**Publisher's note:** Springer Nature remains neutral with regard to jurisdictional claims in published maps and institutional affiliations.

© The Author(s), under exclusive licence to Springer Nature America, Inc. 2019

## Methods

**Yeast strains and plasmids.** Yeast experiments were conducted using the WT haploid strain BY4741 (derived from S288C). For validation of screen results, deletions of *RPS25A* were generated using PCR and homologous recombination to replace each open reading frame with a NatMX resistance cassette to generate the null allele *rps25AΔ::NatMX*. Sense strand *C9orf72* hexanucleotide repeats with (GGGGCC)<sub>25</sub>, (GGGGCC)<sub>40</sub> and (GGGGCC)<sub>66</sub> described previously were used for the present study<sup>21</sup>. The 2- $\mu$ m galactose promoter plasmid pAG426GAL was used for the ribosomal miniscreen and the centromeric galactose promoter plasmid pAG416GAL was used for validations<sup>22</sup>. Cross-validation was performed using pAG426GAL GFP plasmids from the Addgene Yeast Gateway Kit (no. 1000000011)<sup>23</sup>. Plasmids were introduced into yeast strains using standard lithium acetate transformation for individual transformations. For the ribosomal miniscreen, a 96-well transformation was employed<sup>23,24</sup>.

**Yeast lysate preparation and immunoblotting.** For the ribosome miniscreen, overnight yeast cultures grown in 2% raffinose-containing media were diluted into 2% galactose-containing media to induce transgene expression from a 426GAL C9 40R plasmid, and were further grown for 12 h with shaking at 30 °C. For individual validations, yeasts were prepared as above, driving expression from a 416GAL C9 66R plasmid and grown in galactose for 8 h. Yeast cells were harvested by centrifugation (3,000g for 5 min), resuspended in lysis buffer (Y-Per Plus (Thermo Fisher Scientific) and 2X Halt Protease Inhibitor Cocktail (Thermo Fisher Scientific)), and incubated for 20 min at room temperature. Lysates were clarified by centrifugation (10,000g at 4 °C for 10 min) and soluble lysates were subjected to immunoassays.

Yeast protein lysates were quantified using bicinchoninic acid (Pierce BCA) assays and 20  $\mu$ g protein was loaded with 1X NuPAGE LDS sample buffer and 50 mM dithiothreitol, and denatured for 10 min at 70 °C. Samples were loaded on to 4–12% Bis-Tris gels and subjected to polyacrylamide gel electrophoresis. Gels were transferred to 0.45- $\mu$ m nitrocellulose membranes (Bio-Rad) using semi-dry transfer (Bio-Rad Trans-Blot SD Semi-Dry Cell) and 2X, 10% methanol NuPAGE transfer buffer (Novex) at 17 V for 1 h. Membranes were blocked in Odyssey Blocking Buffer and probed with rabbit anti-GFP (1:1,000, Thermo Fisher Scientific A-11122) and mouse anti-glyceraldehyde 3-phosphate dehydrogenase (GAPDH) (1:5,000, Sigma-Aldrich G8795) and horse radish peroxidase (HRP)-conjugated secondary antibodies.

**Yeast RT-qPCR.** For the yeast miniscreen, yeasts were grown as described above. Yeasts were harvested in TRIzol (Thermo Fisher Scientific) and RNA was extracted using a combination of chloroform and the RNA Clean & Concentrator ZR-96 kit (Zymo Research) according to the manufacturer's protocol. RNA, 5  $\mu$ l, was loaded for the RT reaction using the High Capacity cDNA kit (Applied Biosystems) and 1  $\mu$ l of a 1:10 complementary DNA dilution was used for 10  $\mu$ l in qPCR reactions as described below.

RNA was extracted from yeast using a MasterPure Yeast RNA Extraction kit (Epicentre), including DNase I digestions. RNA, 250 ng, was reverse transcribed into cDNA using a High Capacity cDNA Reverse Transcription Kit with random primers (Applied Biosystems). The cDNA products were diluted 1:10 and 2  $\mu$ l was analyzed by qPCR using custom primer sets and SYBR Green reagent (20  $\mu$ l total reaction, PCR Master Mix, Applied Biosystems). The following primers were used: scACT1: forward, 5'-ATTCTGAGGTTGCTGCTTTGG, reverse, 5'-TGTCTTGGTCTACCGACGATAG; C9repeat: forward, 5'-AGCTTAGTACTCGCTGAGGGTG, reverse = 5'-GACTCCTGAGTTCCAGAGCTTG. The 2<sup>- $\Delta\Delta$ Ct</sup> method was used to determine the relative mRNA expression of each gene.

**Poly(GP) ELISA.** Poly(GP) levels in lysates were measured in a blinded fashion using a previously described sandwich immunoassay that uses Meso Scale Discovery electrochemiluminescence detection technology, and an affinity-purified rabbit polyclonal poly(GP) antibody (Rb9259) as both a capture and a detection antibody<sup>25–28</sup>. Lysates were diluted to the same concentration using Tris-buffered saline (TBS) and tested in duplicate wells. Response values, corresponding to the intensity of emitted light on electrochemical stimulation of the assay plate using the Meso Scale Discovery QuickPlex SQ 120, were acquired. All responses were background corrected using the response from the negative control samples. In some cases, when comparing across mutants or iPSC lines, poly(GP) responses were then normalized to the positive control.

**Poly(GR) ELISA.** GR Meso Scale Discovery (MSD) immunoassays were performed as previously described using an affinity-purified rabbit polyclonal anti-GR antibody<sup>29</sup> with the following modification: cells were lysed in radioimmunoprecipitation assay buffer containing 0.5 M urea and 2X protease inhibitors (Roche cComplete Mini ethylenediaminetetraacetic acid free) and 180  $\mu$ g protein loaded per well.

**Yeast anti-GFP ELISA.** The yeast ribosomal mutants were counter-screened for the effect on levels of enhanced GFP (eGFP) in the context of a Kozak sequence and ATG initiation as a readout of general effects on translation. Yeast cells were

induced with galactose and lysed as previously described. Lysates were diluted 1:50 to fit in the range of detection and the manufacturer's protocol was followed without changes (Abcam, ab175181). Signal from mutants expressing eGFP divided by total micrograms of protein loaded for the ELISA was normalized as a ratio of WT eGFP expression and compared with the effect of mutants on poly(GP) expression.

**Mammalian cell culture and treatments.** Hap1 WT and RPS25 KO cell lines<sup>12</sup> were cultured in standard conditions using Iscove's Modified Dulbecco's medium (Thermo Fisher Scientific) with 10% FBS and penicillin–streptomycin. HeLa cell lines were cultured similarly in Dulbecco's modified Eagle's medium (DMEM) (Thermo Fisher Scientific). For *C9orf72* GGGGCC transfections, mammalian expression vectors were used under CAG promoter, empty cassette or GGGGCC<sub>2</sub> or GGGGCC<sub>66</sub> (C9 2R and C9 66R) and with three epitope tags per frame. Transfections of these plasmids were performed with Lipofectamine 3000 (Thermo Fisher Scientific) using the manufacturer's protocol. After 12 h of transfection, the medium was replaced with fresh Iscove's Modified Dulbecco's medium. Hygromycin (300  $\mu$ g  $\mu$ l<sup>-1</sup>, Invivogen) was added at 24 h for selection and cells were harvested 72 h after transfection.

**ATXN2 RAN construct generation.** Variable-length CAG repeats (22, 31, 39, 58, 108 repeat length) were cloned from human *ATXN2* cDNA and subsequently subcloned into a pCDNA6-myc-His-A expression vector using standard molecular cloning techniques (the C' myc-6xHis epitope tags in frame with the poly(A) encoding the forward-reading frame). Then, 38 basepair (bp) upstream and 98 bp downstream of the CAG repeats in the human *ATXN2* gene were included in the construct. All ATG codons upstream of the CAG repeat region identified in any forward reading frame were mutated from ATG to AAG using site-directed mutagenesis (Agilent, QuikChange II Site-Directed Mutagenesis Kit), or the mutations were introduced with primers during PCR. Constructs were verified by Sanger sequencing before transfection.

**HeLa RPS25 KD mutant generation.** Two RPS25 guides were cloned and lentivirus was generated as described previously<sup>27</sup>. HeLa Cas9 cells were subsequently treated with zeocin to select for RPS25-guide-infected cells. Cells were subsequently subcloned and screened via immunoblotting to find the RPS25 KD clone used in the present study. The RPS25 guide sequence provided by the Bassik laboratory was: CACCGTGTCCAAAGGCCAAAGTTC. The RPS25 guide sequence generated using Benchling software was: CACCGCTTCTTTTTGGCCTTGCCCC. HeLa control cells used in the experiments were derived from the same original HeLa Cas9-BFP population and infected with guides containing a safe, non-gene-targeting sequence provided by the Bassik laboratory. The safe guide sequence was: GTCCCCCTCAGCCGTATT.

**Mammalian cell RT-qPCR.** Plates with 24 wells containing Hap1 or HeLa WT or mutant cell lines were harvested using the PureLink RNA Mini Kit (Life Technologies) following the manufacturer's protocol. RNA, 250–500 ng, was used for reverse transcription into cDNA using the High Capacity cDNA Reverse Transcription Kit (Thermo Fisher Scientific). The cDNA was subsequently diluted 1:10 and 2  $\mu$ l was analyzed using qPCR with custom primer sets and SYBR Green reagent (PCR Master Mix, Applied Biosystems). Primers used were: C9repeat: forward, 5'-AGCTTAGTACTCGCTGAGGGTG, reverse, 5'-GACTCCTGAGTTCCAGAGCTTG; hActin (ActB): forward, ATCTGAGGTTGCTGCTTTGG, reverse, TGTCTTGGTCTACCGACGATAG; ATXN2 construct: forward, TCCTCTCTAGAGGGCCCTTC, reverse, TCAATGGTGATGGTGATG; HTT construct: forward, GCAGGCACAGCCGCTGCTGC, reverse, GGTCGGTGACGGCTCCTC; 18S: forward, AGAAACGGCTACCACATCCA, reverse, CACCAGACTTGCCCTCCA; rLuc: forward, TGGAGAATAACTTCTTCGTGGA, reverse, TTGGACGACGAACCTTACC. The 2<sup>- $\Delta\Delta$ Ct</sup> method was used to determine the relative mRNA expression of each gene.

**Mammalian cell lysate preparation and immunoblotting.** Hap1 or HeLa cells were transfected and treated as above before lysis. Cells were washed twice in ice-cold 1X phosphate-buffered saline (PBS) and lysed in ice-cold radioimmunoprecipitation assay buffer supplemented with 1X HALT Protease Inhibitor cocktail (Pierce). Lysate was clarified at 10,000g for 10 min at 4 °C, and protein concentration was measured using bicinchoninic acid (Pierce BCA) assays. Protein, 20–25  $\mu$ g was prepared in 1X sodium dodecylsulfate (SDS) buffer and 2.5% 2-mercaptoethanol (Sigma-Aldrich) and denatured for 5 min at 95 °C. Samples were loaded and resolved as previously described. Transfer was conducted as previously described using 0.45- $\mu$ m poly(vinylidene fluoride) activated briefly in 100% methanol (for poly(GA) analysis) and 0.45- $\mu$ m nitrocellulose for all other immunoblotting. Odyssey Blocking Buffer was used to block and for antibody solutions, with the exception of anti-His solutions, which were made using 5% BSA in Tween 20. Antibodies were as follows: rabbit anti-HA (1:1,000, Cell Signaling 3724), mouse anti-GAPDH (1:5,000, Sigma-Aldrich G8795), rabbit anti-RPS25 (Abcam ab102940), mouse anti-HIS (1:1,000, EMD Millipore 05-949), mouse anti-poly(glutamine) (1:1,000, EMD Millipore 5TF1-1C2), rabbit anti-C9orf72

(1:1,000, sc-138763), rabbit poly(GP) (1:1,000, EMD Millipore ABN1358) and rabbit anti-poly(A), C-terminal-specific RAN antibody (1:2,000, generously shared by the laboratory of L. Ranum)<sup>30</sup>. For puromycin-incorporation assay, 0.45- $\mu$ m nitrocellulose was used and antibodies include: mouse anti-puromycin (1:1,000, EMD Millipore MABE343) and mouse anti-GAPDH, which were probed on separate replicate blots. Secondary antibodies include: goat anti-mouse HRP (1:5,000, Fisher 62-6520), goat anti-rabbit HRP (1:5,000, Fisher 31462), goat anti-mouse Alexa Fluor 790 (1:20,000, Fisher A11371) and goat anti-rabbit Alexa Fluor 680 (1:20,000, Fisher A21109).

**Hap1 puromycin-incorporation assay.** Hap1 WT and RPS25 KO cells were treated with 10  $\mu$ g ml<sup>-1</sup> of puromycin for 10 min before lysis and immunoblotting.

**Hap1-Clover (GFP variant) expression via flow cytometry.** The pcDNA3.1 CMV-ATG-Clover constructs were transfected into Hap1 WT and RPS25 KO cells with Lipofectamine 3000. After 48 h of transient transfection, Hap1 cells were dissociated and resuspended in 1X PBS, 2% FBS, 1 mM ethylenediaminetetraacetic acid buffer and analyzed in the FITC channel for GFP expression using a Guava easyCyte Single Sample Flow Cytometer (EMD Millipore). Data were analyzed using FlowJo (v.X 10.0.7r2) and the mean GFP signal was calculated.

**Hap1 growth curve analysis.** Hap1 WT and RPS25 KO cells were seeded at  $1.5 \times 10^5$  cells into a 12-well plate and imaged with a 10 $\times$  objective every 4 h using the InCuCyte (Essen BioScience). Phase-contrast images were analyzed using the InCuCyte default analysis software to compute percentage confluency. The technical replicate average was determined over nine images collected throughout each well at each time point, to account for differences in growth depending on image point within plates. The biological average across independent wells is plotted in Supplementary Fig. 2. The area-under-the-curve calculations and statistics were performed using the GraphPad Prism analysis option for area under the curve.

**Ribosome fractionation and RT-qPCR.** Hap1 WT and RPS25 KO cells transfected with C9 66R plasmid were lysed in lysis buffer (20 mM Tris, pH 7.5, 150 mM NaCl, 15 mM MgCl<sub>2</sub>, 100  $\mu$ g ml<sup>-1</sup> of cycloheximide (Sigma-Aldrich), 1 mM dithiothreitol, 0.5% Triton X-100, 0.1 mg ml<sup>-1</sup> of heparin (Sigma-Aldrich), 8% glycerol, 20 U ml<sup>-1</sup> of TURBO DNase and 200 U ml<sup>-1</sup> of SUPERase<sup>•</sup>In RNase Inhibitor (Invitrogen), 1X Halt Protease and Phosphatase Inhibitor Cocktail (Thermo Fisher Scientific)) and incubated for 30 min at 4 °C. Lysates were clarified by sequential 1,000g and 10,000g spins, taking the supernatant each time. Of the lysate, 200  $\mu$ l was loaded on to a 10–45% sucrose gradient (20 mM Tris, pH 7.5, 100 mM NaCl, 15 mM MgCl<sub>2</sub>, 100  $\mu$ g ml<sup>-1</sup> of cycloheximide, sucrose) and centrifuged for 2.5 h at 40,000g in an SW40 rotor at 4 °C. Gradients were fractionated on a Brandel Gradient fractionator at 30-s fraction intervals. *Renilla* luciferase RNA spike-in was added at 50 pmol per fraction and used as a normalization control. RNA from each fraction was isolated with phenol-chloroform and precipitated using standard isopropanol extraction; 500 ng is loaded into each RT reaction, fractions were pooled and included free ribonucleoproteins, 40S, 60S, 80S, two polysomes and selected fractions from heavy polysomes (as indicated in Supplementary Fig. 3).

**Human iPSC culture and treatments.** Ichida lab lymphocytes from healthy subjects and ALS patients were obtained from the National Institute of Neurological Disorders and Stroke (NINDS) Biorepository at the Coriell Institute for Medical Research and reprogrammed into iPSCs as described previously<sup>18</sup>. Target ALS patient iPSCs were obtained through the NINDS Human Cell and Data Repository. The NINDS Biorepository requires informed consent from patients. Rothstein lab iPSCs were collected from patients at Johns Hopkins Hospital with the patient's consent and de-identification. Control iPSCs derived from fibroblasts from the Pasca lab were collected from patients under informed consent with the approval of the Stanford Human Stem Cell Research Oversight committee. Information on patient-derived iPSCs can be found in Supplementary Table 3.

Matrigel was prepared according to the manufacturer's protocol in DMEM/Nutrient Mixture F-12 (F12), coated on plates and incubated for 1 h. Human control and patient-derived iPSCs were maintained on Matrigel (Corning)-coated plates using mTeSR1 (STEMCELL Technologies Inc.) medium changed every day. The iPSCs were dissociated with Accutase (STEMCELL Technologies Inc.) in the presence of ROCK inhibitor Y-27632 (Sigma-Aldrich) at 10  $\mu$ M overnight.

For siRNA transfections, first siRNA-lipofectamine complexes were prepared. Non-targeting and RPS25-targeting siRNAs (Dharmacon, Smartpool ON-TARGETplus Smartpool: D-001810-10-05 and L-013629-00-0005, respectively) are prepared in the following ratios: for a 24-well plate, 13  $\mu$ l OptiMEM (Thermo Fisher Scientific) with 1.25  $\mu$ l lipofectamine RNAiMAX (Thermo Fisher Scientific). Separately, 13  $\mu$ l OptiMEM is mixed first with 9 pmol siRNA and then with RNAiMAX mixture and incubated for 15 min. The iPSCs were dissociated as previously described and resuspended in 26  $\mu$ l of the siRNA-RNAiMAX mixture prepared above, and incubated at room temperature for 10 min (maximum time is 15 min). Cells and siRNA mixture were then added to Matrigel pre-coated wells with 0.5 ml mTeSR plus Y-27632. Cells are maintained in Y-27632

for 12 h until the media were exchanged for fresh mTeSR. Cells were harvested 72 h post-transfection.

**Human iPSC RNA FISH and quantification.** RNA FISH was performed as previously reported<sup>31</sup>. The iPSCs treated with RNAi as above were grown on Matrigel-coated coverslips, fixed in 4% paraformaldehyde and permeabilized with 0.2% Triton/DEPC-PBS. Slides were dehydrated with a series of ethanol washes and incubated with hybridization solution. Locked nucleic acid probes, to detect sense (/5TYE563/CCCCGGCCCGCCCC) or antisense (/5TYE563/GGGGCCGGGGCCCGGG) C9orf72 repeats, were prepared and diluted to 100 nM. After hybridization, the cells were incubated with the diluted locked nucleic acid probes at 66 °C for 24 h. Cells were then washed and counterstained with Hoechst 33258 (1  $\mu$ g ml<sup>-1</sup>, Thermo Fisher Scientific). Afterwards, the cells were dehydrated with ethanol washes and coverslips were mounted using ProLong Diamond antifade mountant. Images were obtained on a Leica DM16000B inverted fluorescence microscope with a  $\times$ 60 oil immersion objective. To quantify foci, three coverslips per treatment were analyzed and >200 nuclei were counted per coverslip. Counts were used to determine average number of foci per Hoescht-positive nuclei because iPSCs grow in dense colonies and it is difficult to distinguish in which cytoplasm a particular focus resides.

Foci were quantified in an unbiased manner using the MetaXpress granularity software, which detects foci of a determined size range compared with changes in surrounding pixel intensity. Parameters used for this analysis were 2–7 px in diameter and pixel intensity change of 3,500 gray levels. Hoechst-positive nuclei were counted using the Analyze Particle function in Fiji. Briefly, all images across treatments were stacked, converted to 8 bits and thresholded to the same value before the Analyze Particle function to ensure that every image was quantified uniformly across conditions and coverslips.

**Human iPSC and iMN RT-qPCR analysis.** Human iPSCs were treated with siRNAs, and RNA extraction and RT were set up as described above. Human iPSC-derived iMNs were treated with ASOs for 72 h before freezing in TRIzol (Thermo Fisher Scientific), then RNA was extracted using standard TRIzol-chloroform extraction protocols. RT reactions were set up as described above. Custom TaqMan probes for C9orf72 and standard TaqMan probes for hActin (Thermo Fisher Scientific, Hs01060665\_g1) and RPS25 (Thermo Fisher Scientific, Hs01568661\_g1) were used with the TaqMan Universal Master Mix II (Applied Biosystems, 440040). Custom probes were as follows: C9 total isoforms: forward, TGTGACAGTTGGAATGCAGTGA, reverse, GCCACTTAAAGCAATCTCTGTCTTG; C9 expansion isoforms: forward, GGGTCTAGCAAGAGCAGGTG, reverse, GTCTTGGCAACAGCTGGAGAT.

**Drosophila husbandry.** All flies were reared at 25 °C on a 12-h:12-h light:dark cycle at constant humidity and on standard sugar-yeast-agar medium (agar, 15 g l<sup>-1</sup>; sugar, 50 g l<sup>-1</sup>; autolyzed yeast, 100 g l<sup>-1</sup>; nipagin, 100 g l<sup>-1</sup>; and propionic acid, 2 ml l<sup>-1</sup>).

**Drosophila lifespan analysis.** Flies were raised at standard density in 200-ml bottles. After eclosion, flies were allowed to mate for 24–48 h. Females or males of the appropriate genotype were split into groups of 15 and housed in vials containing sugar-yeast-agar medium with or without 200  $\mu$ M RU486 to induce the gene-switch driver. Deaths were scored and flies tipped on to fresh food three times a week. Data are presented as cumulative survival curves, and survival rates were compared using log-rank tests. All lifespans were performed at 25 °C. ElavGS was derived from the original elavGS 301.2 line<sup>31</sup>. UAS-36(GGGGCC) and UAS-36GR lines have been previously described<sup>17</sup>; UAS-RpS25 RNAi lines P{GD10582}v52602 and P{KK107958}VIE-260B were obtained from the Bloomington stock center.

**Drosophila immunoblotting.** Protein samples were prepared by homogenizing in 2X SDS Laemmli sample buffer (4% SDS, 20% glycerol, 120 mM Tris-HCl, pH 6.8, 200 mM dithiothreitol with bromophenol blue) and boiling at 95 °C for 5 min. Samples were separated on pre-cast 4–12% Invitrogen Bis-Tris gels (NP0322), blotted on to a poly(vinylidene fluoride) membrane, blocked in 5% milk in Tween 20 and incubated with anti-GP polyclonal rabbit antibody (1:1,000)<sup>17</sup>, or mouse anti-actin (Abcam ab8224) (1:10,000), followed by HRP-tagged secondary antibody (anti-rabbit HRP, ab6721 or anti-mouse HRP, ab6789, Abcam, 1:10,000). The protein standard used as a molecular weight ladder was MagicMark XP Western Protein Standard (Thermo Scientific, LC5602).

**Drosophila RT-qPCR.** Total RNA was extracted from eight flies per sample using TRIzol (Gibco) according to the manufacturer's instructions. The concentration of total RNA purified for each sample was measured using an Eppendorf biophotometer. Of the total RNA 1  $\mu$ g was then subjected to DNA digestion using DNase I (Ambion), immediately followed by reverse transcription using the SuperScript II system (Invitrogen) with oligo(dT) primers. Quantitative PCR was performed using the PRISM 7000 sequence-detection system (Applied Biosystems), SYBR Green (Molecular Probes), ROX Reference Dye (Invitrogen) and HotStarTaq (Qiagen) by following the manufacturers' instructions. Each sample was analyzed in duplicate and values are the mean of



four independent biological repeats  $\pm$  s.e.m. Primers used were: Rps25: forward, AAATCGAACAGCTGACGTGC, reverse, AAAATACATTTTCAGCGGCTG.

**Conversion of iPSCs into iMNs.** Reprogramming was performed in 96-well plates ( $8 \times 10^3$  cells per well) or 13-mm plastic coverslips ( $3.2 \times 10^4$  cells per coverslip) that were sequentially coated with gelatin (0.1%, 1 h) and laminin (2–4 h) at room temperature. To enable efficient expression of the transgenic reprogramming factors, iPSCs were cultured in fibroblast medium (DMEM + 10% FBS) for at least 48 h and either used directly for retroviral transduction or passaged before transduction for each experiment. Retroviruses encoding the seven iMN factors (*Ngn2*, *Isl1*, *Lhx3*, *Neurod1*, *Ascl1*, *Brn2* and *Myt1l*) in a pMXs backbone were added in 100–200  $\mu$ l fibroblast medium per 96-well well with 5  $\mu$ g ml<sup>-1</sup> of polybrene. For iMNs, cultures were transduced with lentivirus encoding the *Hb9::RFP* reporter 48 h after transduction with transcription factor-encoding retroviruses. On day 5, primary mouse cortical glial cells from P1 ICR pups (male and female) were added to the transduced cultures in glia medium containing MEM (Life Technologies), 10% donor equine serum (HyClone), 20% glucose (Sigma-Aldrich) and 1% penicillin–streptomycin. On day 6, cultures were switched to N3 medium containing DMEM/F12 (Life Technologies), 2% FBS, 1% penicillin–streptomycin, N2 and B27 supplements (Life Technologies), 7.5  $\mu$ M RepSox (Selleck) and 10 ng ml<sup>-1</sup> each of glial cell-derived neurotrophic factor (GDNF), brain-derived neurotrophic factor (BDNF) and ciliary neurotrophic factor (CNTF) (R&D). The iMN and induced dopaminergic neuron cultures were maintained in N3 medium, and changed every other day, unless otherwise noted<sup>15,27,32</sup>.

**Lentivirus production.** All short hairpin RNA (shRNA) and *Hb9::RFP*-encoding lentiviruses were produced as follows: HEK293T cells were transfected at 80–90% confluency with viral vectors containing the genes of interest and viral packaging plasmids (pPAX2 and VSVG for lentivirus) using poly(ethylenimine) (Sigma-Aldrich). The medium was changed 24 h after transfection. Viruses were harvested at 48 and 72 h after transfection. Viral supernatants were filtered with 0.45- $\mu$ m filters and concentrated by incubating with Lenti-X concentrator (Clontech) for 24 h at 4°C and centrifuging at 1,500g at 4°C for 45 min. The pellets were resuspended in 300  $\mu$ l DMEM + 10% FBS and stored at –80°C.

**Survival assay of seven iMN factors.** On day 3 of iMN conversion, the cultures were incubated with scrambled or RPS25-targeting ASOs (9  $\mu$ M) with 5  $\mu$ g ml<sup>-1</sup> of polybrene in N3 media containing DMEM/F12 (Life Technologies), 2% FBS, 1% penicillin–streptomycin, N2 and B27 supplements (Life Technologies), and 10 ng ml<sup>-1</sup> each of GDNF, BDNF and CNTF (R&D). All shRNA constructs were tagged with GFP to enable specific tracking of Dox–NIL iMNs expressing the shRNAs. On day 5, primary mouse cortical glial cells from P1 ICR pups (male and female) were added to the transduced cultures in N3 media containing 7.5  $\mu$ M RepSox (Selleck). *Hb9::RFP* iMNs appeared between day 13 and day 16 after retroviral transduction. RepSox was removed at day 17 and the survival assay was initiated by adding 10  $\mu$ M glutamate to the culture medium for 12 h. Cells were then maintained in N3 medium with neurotrophic factors without RepSox. Longitudinal tracking was performed by imaging neuronal cultures in a Molecular Devices ImageExpress once every 48 h, starting at day 17. Tracking of neuronal survival was performed using SVcell 3.0 (DRVision Technologies). Neurons were scored as dead when their soma was no longer detectable by red fluorescent protein fluorescence. Neuron survival assays were performed in triplicate. To increase clarity, similar numbers of randomly selected neurons from each trial were combined to generate the quantification shown. ASO sequences are as follows: RPS25-549 (ASO no. 2): mG\*mA\*mG\*mU\*mC\*T\*C\*A\*T\*T\*C\*T\*G\*T\*T\*mG\*mC\*mC\*mC\*mA; and RPS25-2349 (ASO no. 1): mG\*mU\*mU\*mG\*mC\*A\*T\*T\*C\*C\*C\*G\*T\*G\*mC\*mC\*mC\*mU\*mC (with phosphothiorate bonds indicated by \* and 2'-O methylation indicated by m (gapmer design from IDT).

**DPR immunocytochemistry.** Control and patient-derived iMNs were treated with ASOs for 72 h and subsequently fixed in 4% paraformaldehyde for 1 h at 4°C,

permeabilized with 0.1% Triton-X/PBS 20 min at room temperature, blocked with 10% donkey serum in 3% BSA/PBS at room temperature for 2 h, and incubated with primary antibodies with 0.3% BSA/PBS at 4°C overnight. Cells were then washed with 0.1% PBS/Tween 20 and incubated with Alexa Fluor secondary antibodies (Life Technologies) in 0.3% BSA/PBS for 2 h at room temperature. To visualize nuclei, cells were stained with DAPI (Life Technologies) or Hoechst and then mounted on slides with Vectashield (Vector Labs). Images were acquired on an LSM 800 confocal microscope (Zeiss). The following primary antibodies were used: rabbit anti-poly(PR) (Proteintech 23979-1-AP, 1:50) and rabbit anti-poly(GR) (Proteintech 23978-1-AP, 1:50). Twenty iMNs were quantified per genotype per condition. For quantifications of poly(GR) and poly(PR) nuclear puncta, the number of nuclear puncta were counted and divided by total nuclear area as outlined in Supplementary Fig. 10.

**Statistics.** Statistical analyses were performed using GraphPad Prism v.7 and Microsoft Excel. Statistical tests included two-tailed, Student's *t*-test, one or two-way analysis of variance (ANOVA) and two-sided log-rank test for survival data. No power analyses were conducted to predetermine sample size, but the sample sizes are consistent with those reported in previous publications<sup>15,17,18,21</sup>. Data distribution was assumed to be normal, but this was not formally tested. No data or animals were excluded from analysis.

**Randomization.** Unless otherwise stated below, samples were not randomized or blinded during experiments or analysis.

For all poly(GP) and poly(GR) ELISAs, researchers were blinded to samples while performing and analyzing ELISA data. Researchers responsible for transfecting and lysing cells were not blinded.

For iPSC foci image quantifications, RNA foci and nuclei were quantified in an automated manner, as described in the methods with no data being removed, and did not require blinding.

For neuron survival assays, >50 neurons were selected for tracking randomly at day 1 of the assay. To select 50 iMNs per condition for analysis, the survival values for 50 cells were selected at random using the RAND function in Microsoft Excel. For other phenotypes, neurons were selected randomly for analysis. The iMN survival times were confirmed by manual longitudinal tracking by an individual who was blinded to the identity of the genotype and condition of each sample. All other quantification was performed by individuals blinded to the identity of each sample.

**Reporting Summary.** Further information on research design is available in the Nature Research Reporting Summary linked to this article.

## Data availability

The data that support the findings of the present study are available from the corresponding author upon request.

## References

- Kramer, N. J. et al. *Science* **353**, 708–712 (2016).
- Alberti, S., Gitler, A. D. & Lindquist, S. *Yeast* **24**, 913–919 (2007).
- Cooper, A. A. et al. *Science* **313**, 324–328 (2006).
- Gietz, R. D. & Schiestl, R. H. *Nat. Protoc.* **2**, 38–41 (2007).
- Gendron, T. F. et al. *Sci. Transl. Med.* **9**, eaai7866 (2017).
- Gendron, T. F. et al. *Acta Neuropathol.* **130**, 559–573 (2015).
- Kramer, N. J. et al. *Nat. Genet.* **50**, 603–612 (2018).
- Su, Z. et al. *Neuron* **83**, 1043–1050 (2014).
- Simone, R. et al. *EMBO Mol. Med.* **10**, 22–31 (2017).
- Banez-Coronel, M. et al. *Neuron* **88**, 667–677 (2015).
- Osterwalder, T., Yoon, K. S., White, B. H. & Keshishian, H. *Proc. Natl Acad. Sci. USA* **98**, 12596–12601 (2001).
- Son, E. Y. et al. *Cell Stem Cell* **9**, 205–218 (2011).

## Reporting Summary

Nature Research wishes to improve the reproducibility of the work that we publish. This form provides structure for consistency and transparency in reporting. For further information on Nature Research policies, see [Authors & Referees](#) and the [Editorial Policy Checklist](#).

### Statistics

For all statistical analyses, confirm that the following items are present in the figure legend, table legend, main text, or Methods section.

- | n/a                                 | Confirmed  |
|-------------------------------------|--|
| <input type="checkbox"/>            | <input checked="" type="checkbox"/> The exact sample size ( $n$ ) for each experimental group/condition, given as a discrete number and unit of measurement  |
| <input type="checkbox"/>            | <input checked="" type="checkbox"/> A statement on whether measurements were taken from distinct samples or whether the same sample was measured repeatedly  |
| <input type="checkbox"/>            | <input checked="" type="checkbox"/> The statistical test(s) used AND whether they are one- or two-sided<br><i>Only common tests should be described solely by name; describe more complex techniques in the Methods section.</i>   |
| <input checked="" type="checkbox"/> | <input type="checkbox"/> A description of all covariates tested  |
| <input type="checkbox"/>            | <input checked="" type="checkbox"/> A description of any assumptions or corrections, such as tests of normality and adjustment for multiple comparisons  |
| <input type="checkbox"/>            | <input checked="" type="checkbox"/> A full description of the statistical parameters including central tendency (e.g. means) or other basic estimates (e.g. regression coefficient) AND variation (e.g. standard deviation) or associated estimates of uncertainty (e.g. confidence intervals) |
| <input type="checkbox"/>            | <input checked="" type="checkbox"/> For null hypothesis testing, the test statistic (e.g. $F$ , $t$ , $r$ ) with confidence intervals, effect sizes, degrees of freedom and $P$ value noted<br><i>Give <math>P</math> values as exact values whenever suitable.</i>                            |
| <input checked="" type="checkbox"/> | <input type="checkbox"/> For Bayesian analysis, information on the choice of priors and Markov chain Monte Carlo settings  |
| <input checked="" type="checkbox"/> | <input type="checkbox"/> For hierarchical and complex designs, identification of the appropriate level for tests and full reporting of outcomes  |
| <input checked="" type="checkbox"/> | <input type="checkbox"/> Estimates of effect sizes (e.g. Cohen's $d$ , Pearson's $r$ ), indicating how they were calculated  |

*Our web collection on [statistics for biologists](#) contains articles on many of the points above.*

### Software and code

Policy information about [availability of computer code](#)

Data collection

Tracking of neuronal survival was performed using SVcell 3.0 (DRVision Technologies). qPCR data was collected using CFX manager (BioRad) and polysome associated A260nm data was collected using PeakChart.

Data analysis

GraphPad Prism version 7.0d was used to plot data and used for statistical analysis. Microsoft Excel version 15.27 was used for log rank test for Drosophila survival curve data. MetaXpress granularity software was used to count foci in RNA FISH experiments. Fiji was used to count nuclei and create immunofluorescence figures. Flow cytometry data was analyzed using Flowjo (version X 10.0.7r2) and the mean GFP signal was calculated.

For manuscripts utilizing custom algorithms or software that are central to the research but not yet described in published literature, software must be made available to editors/reviewers. We strongly encourage code deposition in a community repository (e.g. GitHub). See the Nature Research [guidelines for submitting code & software](#) for further information.

### Data

Policy information about [availability of data](#)

All manuscripts must include a [data availability statement](#). This statement should provide the following information, where applicable:

- Accession codes, unique identifiers, or web links for publicly available datasets
- A list of figures that have associated raw data
- A description of any restrictions on data availability

The data supporting the findings of this study are available from the corresponding author upon reasonable request.

## Field-specific reporting

Please select the one below that is the best fit for your research. If you are not sure, read the appropriate sections before making your selection.

Life sciences  Behavioural & social sciences  Ecological, evolutionary & environmental sciences

For a reference copy of the document with all sections, see [nature.com/documents/nr-reporting-summary-flat.pdf](https://www.nature.com/documents/nr-reporting-summary-flat.pdf)

## Life sciences study design

All studies must disclose on these points even when the disclosure is negative.

Sample size	No power analyses were used to predetermine sample sizes. However, sample sizes were chosen based on prior literature using similar experimental paradigms, or in the case of Drosophila experiments, previous published experimental paradigms.
Data exclusions	No data were excluded from analysis.
Replication	For in vitro experiments, two, independently generated RPS25KO cells in two separate cell lines were used. Biological replicates (separate transformation of cells) were conducted on different days to ensure reproducibility. For patient-derived cell data, multiple control and patient cells were utilized to ensure reproducibility. For Drosophila experiments, flies from multiple, separate crosses were used for analysis. All attempts at replication were successful. Detailed information for every experiment regarding number of times an experiment was repeated or if an experiment was performed only once can be found in Table S4.
Randomization	For neuron survival assays, >50 neurons were selected for tracking randomly at day 1 of the assay. To select 50 iMNs per condition for analysis, the survival values for 50 cells were selected at random using the RAND function in Microsoft Excel. No other randomization was performed.
Blinding	iMN survival times were confirmed by manual longitudinal tracking by an individual who was blinded to the identity of the genotype and condition of each sample. For iMN DPR immunocytochemistry, quantification was performed by individuals blinded to the identity of each sample. Blinding was not performed on patient-derived iPSC RNA FISH because these data were collected or analyzed in an unbiased, automated fashion with predetermined settings applied uniformly to all conditions. Blinding of Drosophila was not possible as flies are genotyped and placed in grouped vials for induction of transgene(s). Immunoassays for poly(GP) and poly(GR) were blinded until after data was collected and analyzed. All other experiments were not blinded.

## Reporting for specific materials, systems and methods

We require information from authors about some types of materials, experimental systems and methods used in many studies. Here, indicate whether each material, system or method listed is relevant to your study. If you are not sure if a list item applies to your research, read the appropriate section before selecting a response.

### Materials & experimental systems

n/a	Involved in the study
<input type="checkbox"/>	<input checked="" type="checkbox"/> Antibodies
<input type="checkbox"/>	<input checked="" type="checkbox"/> Eukaryotic cell lines
<input checked="" type="checkbox"/>	<input type="checkbox"/> Palaeontology
<input type="checkbox"/>	<input checked="" type="checkbox"/> Animals and other organisms
<input checked="" type="checkbox"/>	<input type="checkbox"/> Human research participants
<input checked="" type="checkbox"/>	<input type="checkbox"/> Clinical data

### Methods

n/a	Involved in the study
<input checked="" type="checkbox"/>	<input type="checkbox"/> ChIP-seq
<input type="checkbox"/>	<input checked="" type="checkbox"/> Flow cytometry
<input checked="" type="checkbox"/>	<input type="checkbox"/> MRI-based neuroimaging

## Antibodies

### Antibodies used

Rabbit anti-GFP ThermoFisher Scientific cat.# A-11122, 1:1000; Rabbit polyclonal poly(GP) ab9259; Rabbit anti-HA Cell Signaling cat.# 3724 (C29F4), 1:1000; Mouse anti-GAPDH Sigma cat.# G8795 (GAPDH-71.1), 1:5000; rabbit anti-RPS25 (Abcam ab102940); Mouse anti-HIS EMD Millipore cat.# 05-949 (HIS.H8), 1:1000; Mouse anti-polyGlutamine EMD Millipore cat.# MAB1574 (5TF1-1C2), 1:1000; Rabbit anti-C9orf72 Santa Cruz cat.# sc-138763, 1:1000; Rabbit poly(GP) EMD Millipore cat.# ABN1358, 1:1000; Rabbit anti-poly(A) C-terminal-specific HTT RAN antibody Dr. Laura Ranum, 1:2000; Mouse anti-puromycin EMD Millipore cat.# MABE343 (12D10), 1:1000; Rabbit anti-poly(GP) polyclonal antibody Dr. Adrian Isaacs lab; Rabbit anti-poly(PR) Proteintech cat.# 23979-1-AP, 1:50; Rabbit anti-poly(GR) Proteintech cat.# 23978-1-AP, 1:50; rabbit polyclonal anti-GR antibody Dr. Adrian Isaacs Lab, 1:1000. Secondary antibodies include: goat anti-mouse HRP (1:5000, Fisher cat.# 62-6520), goat anti-rabbit HRP (1:5000, Fisher cat.# 31462), goat anti-mouse Alexa Fluor 790 (1:20,000, Fisher cat.# A11371), and goat anti-rabbit Alexa Fluor 680 (1:20,000, Fisher cat.# A21109). For Drosophila experiments, mouse anti-actin Abcam cat.# ab8224, 1:10000; anti-rabbit HRP, Abcam cat.# ab6721 or anti-mouse HRP, Abcam cat.# ab6789, 1:10,000.

### Validation

All commercial antibodies were validated by manufacturer, as follows: anti-RPS25 ab102940 (<https://www.abcam.com/rps25-antibody-ab102940.html> and Fuchs et al. 2015), CRISPR-induced

knockout and exogenously expressed RPS25-HA tag were used to confirm antibody specificity. Anti-GFP, A-11122 (<https://www.thermofisher.com/antibody/product/GFP-Antibody-Polyclonal/A-11122>), plus or minus GFP transfections into human HeLa cells, positive signal at the correct molecular weight only in GFP-transfected cells by Western blotting. Reacts to exogenous tag, so will work across species.

Cell Signaling, anti-HA #3724 (<https://www.cellsignal.com/products/primary-antibodies/ha-tag-c29f4-rabbit-mab/3724>), only HeLa cells transfected with HA-tagged gene are immunoreactive by Western blotting. Reacts to exogenous tag, so will work across species.

anti-GAPDH Sigma cat.# G8795 (<https://www.sigmaaldrich.com/catalog/product/sigma/g8795?lang=en&region=US>), cross species reactivity including human, mouse, and yeast immunoreactive by Western blot with positive signal at correct molecular weight.

anti-HIS EMD Millipore cat.# 05-949 ([http://www.emdmillipore.com/US/en/product/Anti-Histidine-Tagged-Antibody-clone-HIS.H8,MM\\_NF-05-949#anchor\\_COA](http://www.emdmillipore.com/US/en/product/Anti-Histidine-Tagged-Antibody-clone-HIS.H8,MM_NF-05-949#anchor_COA)) only HeLa cells transfected with His-tagged gene are immunoreactive by Western blotting. Reacts to exogenous tag, so will work across species.

Mouse anti-polyglutamine EMD Millipore cat.# MAB1574 ([http://www.emdmillipore.com/US/en/product/Anti-Polyglutamine-Expansion-Diseases-Marker-Antibody-clone-5TF1-1C2,MM\\_NF-MAB1574#anchor\\_DS](http://www.emdmillipore.com/US/en/product/Anti-Polyglutamine-Expansion-Diseases-Marker-Antibody-clone-5TF1-1C2,MM_NF-MAB1574#anchor_DS) and Trottier et al. 1995, Nature). In our paper, in figures 2 and S3, we include an empty control to illustrate specificity of the polyQ signal. Specificity: human.

anti-C9orf72 Santa Cruz cat.# sc-138763 (Jung et al. eLIFE, 2017), specificity human, IP-mass spec and exogenous expression of C9orf72. poly(GP) EMD Millipore cat.# ABN1358 [http://www.emdmillipore.com/US/en/product/Anti-C9ORF72-C9RANT-Poly-GP-sense-antisense,MM\\_NF-ABN1358?ReferrerURL=https%3A%2F%2Fwww.google.com%2F#anchor\\_COA](http://www.emdmillipore.com/US/en/product/Anti-C9ORF72-C9RANT-Poly-GP-sense-antisense,MM_NF-ABN1358?ReferrerURL=https%3A%2F%2Fwww.google.com%2F#anchor_COA)) Evaluated by Western Blotting in transfected HEK293 cell lysate.

anti-puromycin EMD Millipore cat.# MABE343 ([http://www.emdmillipore.com/US/en/product/Anti-Puromycin-Antibody-clone-12D10,MM\\_NF-MABE343#anchor\\_COA](http://www.emdmillipore.com/US/en/product/Anti-Puromycin-Antibody-clone-12D10,MM_NF-MABE343#anchor_COA)). Evaluated by Western Blotting in HEK293 cell lysates treated with Puromycin and Cyclohexamide, or with Puromycin only.

anti-poly(PR) Proteintech cat.# 23979-1-AP (Wen et al. 2014, Neuron) ICC in cells expressing or not expressing PR.

anti-poly(GR) Proteintech cat.# 23978-1-AP (<https://www.ptglab.com/products/GR-repeat-Antibody-23978-1-AP.htm>). Recombinant protein was tested via immunoblotting with this antibody.

anti-actin Abcam cat.# ab8224 (<https://www.abcam.com/beta-actin-antibody-mabcam-8224-loading-control-ab8224.html>), Detects a band of approximately 42 kDa (predicted molecular weight: 42 kDa). Can be blocked with Human beta Actin peptide (ab13772).

WB: A431; HEK293; NIH3T3; PC12 whole cell lysates; Xenopus embryo lysate; Drosophila lysate; S. pombe lysate. Flow Cyt: HeLa cells. ICC/IF: Panc-1 cells; Human fibroblasts.

Antibodies validated by research groups: Rabbit polyclonal poly(GP) ab9259 (Generated and validated by researchers in Gendron et al. 2015, Gendron et al. 2017); Rabbit anti-poly(A) C-terminal-specific HTT RAN antibody Dr. Laura Ranum (Generated and validated by researchers in Banez-Coronel et al. 2015); Rabbit anti-poly(GP) polyclonal antibody Dr. Adrian Isaacs lab (generated and validated in Mizielinska et al. 2014); rabbit polyclonal anti-GR antibody (Simone et al 2018).

## Eukaryotic cell lines

Policy information about [cell lines](#)

Cell line source(s)

HeLa-Cas9-BFP (Dr. Michael Bassik's lab, Stanford University)  
Hap1 Wildtype, RPS25KO and RACK1KO (Dr. Joseph Puglisi's lab, Stanford University)

Authentication

Cell line authentication was originally performed by the supplier, but not independently authenticated in gifting lab or our lab. HeLa-Cas9BFP cells were received from Dr. Michael Bassik and Hap1 cells were received from Dr. Joseph Puglisi. Validations by supplier are performed by PCR, sanger sequencing or exome-sequencing and details can be found as follows: Hap1 (<https://www.horizondiscovery.com/cell-lines/all-products/isogenic-cell-lines/cell-line-faq#D>, see "validation") and HeLa (<https://www.atcc.org/en/Products/All/CCL-2.aspx#documentation>, see "Certificate of analysis").

Mycoplasma contamination

Cells were not tested for mycoplasma contamination by our lab.

Commonly misidentified lines  
(See [ICLAC](#) register)

Cells lines were not listed in ICLAC register.

## Animals and other organisms

Policy information about [studies involving animals](#); [ARRIVE guidelines](#) recommended for reporting animal research

Laboratory animals

The following Drosophila strains were used in this study (males and females): ElavGS was derived from the original elavGS 301.2 line30 and obtained as a generous gift from Dr. H. Tricoire (CNRS). UAS-36(GGGGCC) and UAS-36GR lines published in Mizielinska et al. 2014, UAS-Rps25 RNAi lines P{GD10582}v52602 and P{KK107958}VIE-260B were obtained from Bloomington stock center. JAX-009122 (mice): Post-natal day 2 was used for glial cell dissection.

Wild animals

This study did not involve wild animals.

Field-collected samples

This study did not involve field-collected samples.

Ethics oversight

No ethical approval was required for Drosophila studies. All mouse procedures were performed in agreement with the National Institutes of Health Guide for the Care and Use of Experimental Animals, approved by University of Southern California Institutional Animal Care and Use Committee (11938).

Note that full information on the approval of the study protocol must also be provided in the manuscript.

# Flow Cytometry

## Plots

Confirm that:

- The axis labels state the marker and fluorochrome used (e.g. CD4-FITC).
- The axis scales are clearly visible. Include numbers along axes only for bottom left plot of group (a 'group' is an analysis of identical markers).
- All plots are contour plots with outliers or pseudocolor plots.
- A numerical value for number of cells or percentage (with statistics) is provided.

## Methodology

Sample preparation

Hap1 cells were dissociated and resuspended in 1X PBS, 2% FBS, 1mM EDTA buffer and analyzed in the FITC channel for GFP expression using a Guava easyCyte Single Sample Flow Cytometer (EMD Millipore). Data was analyzed using Flowjo (version X 10.0.7r2) and the mean GFP signal was calculated.

Instrument

Guava easyCyte Single Sample Flow Cytometer (EMD Millipore)

Software

Data was analyzed using Flowjo (version X 10.0.7r2).

Cell population abundance

No sorting was conducted, GFP+ cells were quantified.

Gating strategy

No sorting was conducted, GFP+ cells were determined by comparing FITC vs. cell number histograms using a cell population negative for GFP.

- Tick this box to confirm that a figure exemplifying the gating strategy is provided in the Supplementary Information.